

# AERO-VIS: Asynchronous Event-based Real-time Onboard Visual-Inertial SLAM

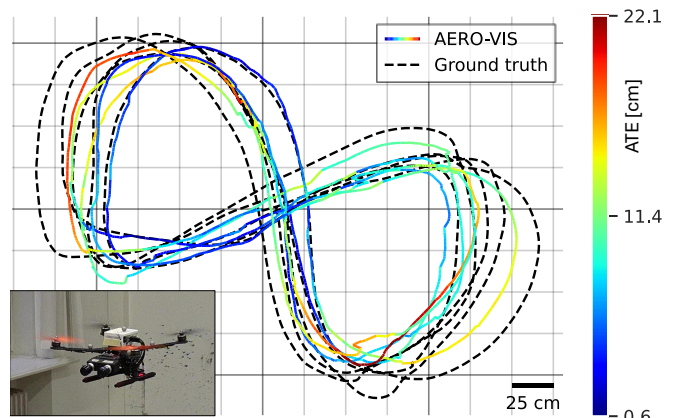
Yannick Burkhardt<sup>1,2,3</sup>, Sebastián Barbas Laina<sup>1,2,4</sup>, Simon Boche<sup>1,2</sup>, Leonard Freißmuth<sup>1</sup>, Stefan Leutenegger<sup>1</sup>

**Abstract**—The robustness of event cameras to high dynamic range and motion blur holds the potential to improve visual odometry systems in challenging environments. Although their high temporal resolution does not require synchronous processing, most event-based odometry methods still run at fixed rates, which simplifies system design but restricts latency and throughput. In this work, we present AERO-VIS, a stereo event-inertial SLAM system with an integrated, data-driven, robust, and performance-optimized keypoint detector. By processing the event stream asynchronously, the system dynamically adapts to downstream runtime demands, ensuring low-latency and real-time performance. When deploying AERO-VIS on a UAV, we achieve unprecedented accuracy in onboard event-based SLAM. These unique characteristics enable us to present the first purely event-based inertial SLAM system that demonstrates closed-loop UAV control and large-scale state estimation while relying solely on onboard compute. A video of the experiments and the source code are available at [ethz-mrl.github.io/AERO-VIS](https://github.com/ethz-mrl/AERO-VIS).

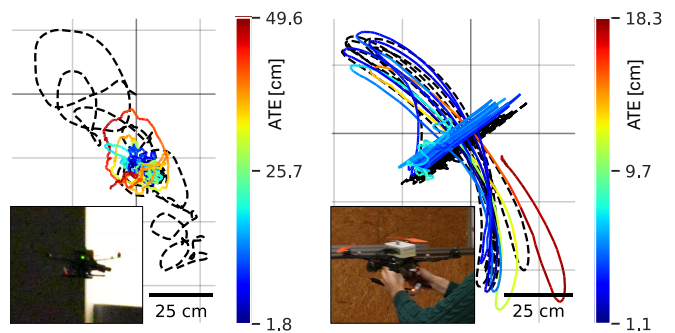
## I. INTRODUCTION

Visual odometry (VO) and SLAM systems provide the essential localization and mapping capabilities required for fully autonomous robotic navigation. However, the reliability of these systems can be compromised by the inherent limitations of traditional frame-based sensors in high-speed or low-light environments. By providing high dynamic range (HDR) and microsecond-level temporal precision resistant to motion blur, event cameras enhance robotic perception in extreme conditions where traditional frame cameras often fail. However, the transition from synchronous frames to asynchronous, sparse event streams demands the development of entirely new algorithmic frameworks capable of handling non-traditional data. The lack of efficient event data processing paradigms forces most current event-based visual VO and SLAM systems to choose between high accuracy and real-time performance. These developments often led to a dependence on large power-hungry computational resources in current state-of-the-art (SOTA) systems [1]–[3] – a requirement that cannot be satisfied on most mobile robot platforms, such as unmanned aerial vehicles (UAVs).

A few systems have been evaluated onboard UAVs [4], [5], but these fall short in terms of accuracy and stability. Consequently, they remain insufficient for the rigorous demands



(a) Closed-loop control under normal conditions.



(b) Closed-loop control in HDR scenario where frame-based estimation fails.

(c) Aggressive handheld motion with velocities up to 3 m/s and 270 °/s.

Fig. 1: Estimated trajectories by AERO-VIS when employed onboard a UAV.

of closed-loop control and high-level autonomy in real-world scenarios. The high event rate triggered by drone vibrations and aggressive motion poses an additional challenge for onboard systems with a limited real-time budget. With this paper, we therefore aim to answer the research question: *Can a UAV be successfully controlled relying on event cameras as the only visual sensing modality?*

Addressing this challenge requires an event-based system capable of accurate and efficient pose estimation. Therefore, we modify the SOTA frame-based visual-inertial (VI) SLAM system OKVIS2 [6] and employ a data-driven approach to detect and describe keypoints in the event stream, inspired by [1]. By improving the Multi-Channel Time Surface (MCTS) event representation and streamlining the network architecture, our resulting model enhances tracking accuracy

<sup>1</sup>Mobile Robotics Lab, ETH Zürich,  
{yannick.burkhardt,sebastian.laina,simon.boche,  
leonard.freissmuth,stefan.leutenegger}@mrl.ethz.ch

<sup>2</sup>Technical University of Munich,

<sup>3</sup>Munich Center for Machine Learning (MCML),

<sup>4</sup>Munich Institute of Robotics and Machine Intelligence (MIRMI)

while significantly reducing the computational requirements. Unlike frame-based cameras, the event stream provides near-continuous temporal information. We exploit this property by designing an asynchronous system that operates at the maximum rate supported by the computational resources, effectively minimizing latency while maximizing throughput.

Our stereo event-inertial SLAM system, AERO-VIS, achieves superior estimation accuracy on public datasets while running in real-time on an NVIDIA Jetson Orin NX, outperforming state-of-the-art approaches [2], [3] that operate without computational constraints. In several real-world experiments, we further validate AERO-VIS’s precision and stability. We demonstrate that our system retains the event camera’s inherent robustness to HDR illumination and its immunity to motion blur during aggressive drone movement, as visualized in Fig. 1. Additionally, it preserves the robust large-scale trajectory estimation and loop-closure capabilities of OKVIS2.

**Contributions:** (1) We present AERO-VIS, an event-based SLAM system designed to maximize processing frequency and minimize latency through an asynchronous architecture, extending the OKVIS2 [6] framework. (2) We introduce a refined event representation and a streamlined architecture for a SOTA [1] keypoint detector and descriptor, simultaneously improving its accuracy and achieving a ten-fold reduction in its onboard inference time. (3) Extensive experiments demonstrate AERO-VIS’s robustness and efficiency across multiple public datasets and in real-world scenarios with fast motion, high dynamic range, or large scale. To our knowledge, this work marks the first successful demonstration of a closed-loop UAV control system driven by event-based sensing.

## II. RELATED WORK

In this section, we review event-based VO and SLAM approaches grouped in feature-based, direct, and data-driven methods, with a special focus on their real-time capability.

**Feature-based methods** attempt to find the same keypoints, e.g., corners, in multiple temporal instances of a scene to infer the camera motion. The early monocular EVIO [7] tracks features in event-frames by compensating for camera motion with local optical flow, subsequently fusing estimates via an extended Kalman filter. Since runtime scales linearly with feature count, the system becomes inefficient during high-density tracking required for stable estimation. Another monocular approach [8] estimates the camera pose change by matching time-surface [9] patches around Arc\* corners [10] via cross-correlation. However, the motion-dependent features cause instability during motion changes, while Arc\*’s event-by-event processing creates computational overhead that limits real-time onboard use. By leveraging line features, the monocular system [11] employs EMVS [12] for mapping and a Lie-formulated error-state Kalman filter for pose estimation. It achieves high processing rates but limited robustness and accuracy.

ESVIO [4] utilizes a stereo event-inertial setup, with optional support for stereo frame cameras. Building on its

monocular predecessor [13], the system leverages gyroscope data to compensate for rotational motion, aligning events in the image plane. Arc\*-detected corners are tracked with the Lukas-Kanade method [14] and fused with frame-based matches. While the full ESVIO pipeline – integrating both frame and event data – is validated through real-time, closed-loop UAV control, the event-only configuration lacks similar hardware validation. Its inferior performance on standard datasets compared to other event-based solutions [2], [3] suggests that ESVIO’s stability is fundamentally tied to the inclusion of frame-based input rather than the event stream alone.

**Direct methods** infer the camera motion by aligning events densely. The first work to achieve 6D event camera pose tracking [15] estimates log-intensity images to estimate depth and camera motion under the constant-brightness assumption. It leverages a GPU to achieve real-time estimation with low-resolution event cameras. EVO [16] increases efficiency by estimating camera motion and a semi-dense map through geometric alignment of binary event frames. However, both of these monocular approaches show limited accuracy and robustness compared to modern methods [2], [3].

ES-PTAM [17] employs MC-EMVS [18], a multi-camera mapping framework that optimizes the ray reprojection of events observed from different camera views, along with edge-map alignment for pose estimation. In addition to significant drift in the evaluation results, the system requires the ground truth pose for initialization, severely limiting its usability in real-world scenarios.

The stereo event-based system ESVO [19] optimizes the spatio-temporal consistency of time surfaces for localization and mapping. While one work extends ESVO to use truncated signed distance functions for mapping [20], several others incorporate IMU measurements: [21] improves event alignment by motion compensation, and two consecutive approaches of the ESVO authors [2], [22] introduce a tightly coupled optimization of inertial and event data, alongside a refined event representation via edge pixel sampling. The resulting system, ESVO2 [2], achieves SOTA efficiency, processing VGA-resolution event streams in real-time on a modern desktop PC.

**Data-driven methods** employ deep learning to obtain a statistical model capable of predicting the camera pose (end-to-end) or to tackle a sub-problem, e.g., keypoint detection (hybrid). Some self-supervised end-to-end learning approaches predict monocular optical flow, depth, and ego-motion [23], [24] but struggle to generalize beyond the specific driving scenarios encountered during training.

DEVO [25] attempts to overcome this limitation by adapting the monocular, frame-based end-to-end model DPVO [26] to the event domain, introducing a patch selection mechanism and training on a large synthetic dataset. The promising results suffer from scale ambiguity, an inherent limitation of monocular systems. Two approaches address this problem by extending DEVO to additional sensors. DEIO [27] additionally incorporates inertial measurements,

however, its metric-scale estimation remains unstable. Rather than relying on an IMU, SDEVO [3] employs a novel static stereo association method to recover metric scale through stereo event cameras. While both DEVO and DEIO are not real-time optimized, SDEVO streamlines data processing and employs a mixed-precision model to operate at 15 Hz at VGA resolution on a desktop PC with a modern GPU.

A hybrid monocular VIO system [5] reconstructs frames from the event stream with the efficient, data-driven FireNet [28] and processes them with OpenVINS [29]. Its lightweight components allow onboard pose estimation at 20 Hz. However, frame reconstruction can produce artifacts, introduces computational overhead and neutralizes the high temporal resolution of event cameras.

Recently, the data-driven method SuperEvent [1] emerged to improve the robustness of event-based keypoint detection and description. It adapts SuperPoint [30] to the event domain by employing the MCTS event representation, a multi-channel generalization of time surfaces to mitigate their dependence on scene motion. The authors achieve promising event-based benchmarking results by replacing the frame-based detector of the VI-SLAM system OKVIS2 [6] with SuperEvent. However, like most data-driven methods, it lacks real-time capability and relies on synchronous processing at a fixed, predefined rate. In this work, we build on this approach by improving SuperEvent’s accuracy and performance, streamlining data flow, and adapting the OKVIS2 framework for asynchronous real-time processing to achieve real-world onboard estimation.

### III. METHOD

AERO-VIS introduces several key innovations. As the system relies on keypoint matching, it necessitates a highly accurate and efficient method for event-based keypoint detection and description. To meet this requirement, we leverage SuperEvent [1], based on an enhanced input representation as detailed in Sec. III-A. Furthermore, to accommodate the limited computational resources of embedded hardware, we introduce the runtime-optimized network architecture of SuperLitE in Sec. III-B before presenting the asynchronous AERO-VIS framework in Sec. III-C.

#### A. Multi-Channel Time Surfaces with Constant Event Count

MCTSs are a generalization of time surfaces to more than one channel, which have shown to improve the prediction stability of keypoint detection networks [1]. A key limitation of traditional time surfaces is their sensitivity to the time window parameter, as its ideal setting varies with the local motion of individual keypoints. To enrich the information for the neural network, the MCTS stacks polarity-separated time surfaces for  $K$  different time window durations  $\Delta t_k$ . These define the  $2K$  sets of events  $\mathcal{E}_{p,\Delta t_k} = \{\mathbf{e}_i \mid p_i = p, t_i \in [\tau - \Delta t_k, \tau]\}$  at time  $\tau$  with each event  $\mathbf{e}_i = (t_i, x_i, y_i, p_i)$  characterized by its timestamp  $t_i$ , pixel coordinates  $(x_i, y_i)$ , and polarity  $p_i \in \{-1, +1\}$ . The MCTS tensor at  $\tau$  is

computed as

$$\text{MCTS} = (\mathbf{TS}_{-1,\Delta t_1}, \dots, \mathbf{TS}_{-1,\Delta t_K}, \mathbf{TS}_{+1,\Delta t_1}, \dots, \mathbf{TS}_{+1,\Delta t_K}), \quad (1)$$

with the zero-initialized time surfaces TS

$$\mathbf{TS}_{p,\Delta t_k}(x_i, y_i) = \max_{\mathbf{e}_i \in \mathcal{E}_{p,\Delta t_k}} \left(1 - \frac{\tau - t_i}{\Delta t_k}\right). \quad (2)$$

While SuperEvent shows promising results in keypoint detection and description, the event stream’s motion dependence limits performance for strong motion changes. Even though the motion-dependent appearance of features is an inherent property of the event camera, the described problem can be mitigated by reformulating the MCTS calculation. Instead of using fixed time windows  $\Delta t_k$ , we propose to adapt  $\Delta t_k$  to obtain a constant number of events  $N_{e,k}$  per channel pair  $k$

$$\Delta t_k = \tau - t_{I-N_{e,k}}, \quad (3)$$

with the index  $I$  for the most recent event. This results in visually more similar time surfaces for varying motion magnitudes, allowing for improved keypoint predictions as shown in Sec. IV-A. We denote the MCTS formulation introduced in SuperEvent [1] as  $\text{MCTS}_{\Delta t}$  and our proposed version as  $\text{MCTS}_{N_{e,k}}$ , highlighting which property is kept constant. In contrast to the five time windows of  $\text{MCTS}_{\Delta t}$  in SuperEvent, we empirically observe that four logarithmically-distributed  $N_{e,k}$  (yielding an eight-channel input tensor) carry sufficient information – further increasing the temporal range does not show accuracy improvements. To ensure sensor-agnosticism, we normalize the event counts  $N_{e,k}$  by the total number of sensor pixels as the event rate scales with spatial resolution. This yields normalized event counts  $\bar{N}_{e,k} \in \{0.03, 0.1, 0.3, 1.0\}$  events/pixel. In the following, *SuperEvent+* refers to this refined approach, which maintains the original SuperEvent architecture with an adjusted first layer to process the eight-channel  $\text{MCTS}_{N_{e,k}}$  input tensor.

#### B. SuperLitE Architecture

Achieving real-time performance on embedded hardware requires a highly efficient and computationally lightweight network architecture. Our analysis revealed that shared encoder and descriptor processing constitute the primary computational bottlenecks within the SuperEvent [1] architecture. We conducted a design space search to identify the most efficient model, varying the encoder architectures [31]–[33] and adapting both the network depth and descriptor dimensionality. We find that an encoder with four layers, each with one convolution, maximum-pooling, and batch-normalization, is sufficient to maintain good accuracy while drastically accelerating onboard inference. Additionally, reducing the descriptor dimensionality from 256 to 64 facilitates faster interpolation of the spatially-reduced descriptor map and accelerates data transfer and matching operations within our SLAM system. We name the resulting, performance-optimized model *SuperLitE*, where the trailing “E” emphasizes its *Event* processing capability.

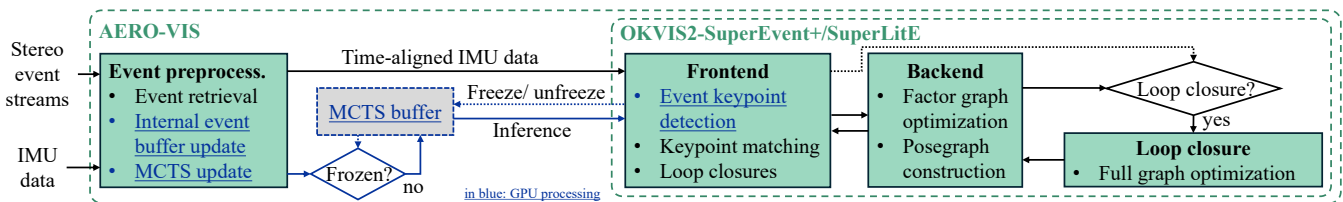


Fig. 2: Stereo event and IMU data are preprocessed through time synchronization and high-frequency MCTS calculation in a shared buffer. The frontend processes this buffer asynchronously, freezing it for SuperLitE inference directly after completing the previous iteration’s keypoint matching and loop closure detection. The backend optimizes the factor graph of recent sensor observations and constructs the posegraph on every new keyframe. If a loop closure is detected, a detached thread is initiated to re-optimize the global pose graph in the background.

### C. AERO-VIS System Design

OKVIS2 [6] employs keypoint matching for landmark triangulation and residual computation within the frontend thread, while the backend utilizes factor-graph optimization to jointly estimate camera poses and landmark positions. Loop closures are detected in the frontend by comparing the current set of descriptors with previous keyframes encoded in a DBoW2 [34] database. To ensure robustness against false positives, heuristic checks verify that drift remains within realistic bounds before triggering a full factor graph optimization in a detached background thread.

To achieve event-inertial SLAM, we modify the OKVIS2 framework by substituting its conventional frame-based keypoint detector with one of our event-based approaches. Depending on available computational resources and runtime constraints, the system can be configured to use either the full SuperEvent+ model or its runtime-optimized variant, SuperLitE. Additionally, we adjust the calculation of the descriptor distance. Instead of the Euclidean distance employed in [1], we use the cosine distance, as it reduces the required computations per matching attempt.

In practice, the system’s per-iteration processing time is dynamic, scaling with operational factors such as the number of observed keypoints and the growing historical depth of the keyframe database. Additionally, the near time-continuous event stream allows state estimation at any given timestamp by generating and processing the corresponding  $MCTS_{Ne}$ . Exploiting this property, our idea is to process the latest possible event state when the frontend is ready. This reduces the system’s latency compared to synchronous (e.g., frame-based) processing.

On devices with limited computational resources, creating an  $MCTS_{Ne}$  comes with significant computational cost. To avoid unnecessarily reducing the system’s throughput, we decouple event preprocessing from state estimation. For multi-modal alignment, only events with corresponding IMU data are processed, while newer events are retained in a buffer. These synchronized events update a two-channel GPU-tensor, storing the most recent event timestamps per pixel and polarity. This tensor then serves as the basis for calculating the  $MCTS_{Ne}$  within shared memory. The frontend thread gates this memory, permitting updates only when the memory is not utilized for inference.

The preprocessing thread is aligned with the event sensor’s fixed, high-frequency event stream update rate to ensure minimal frontend latency. To maximize throughput, the thread decoupling allows the remaining SLAM system to run asynchronously. Whenever the frontend thread finished the previous iteration, it freezes the shared MCTS buffer to run SuperLitE inference, and then unfreezes it again. After keypoint selection, the resulting normalized descriptors are quantized from floating-point to 8-bit integers, allowing for more efficient copying and calculations. We apply symmetric min-max quantization using a scaling factor derived from the training data. This factor is neutralized during cosine distance calculation.

A block diagram of our system *AERO-VIS* can be found in Fig. 2. The system is real-time capable by design, since its asynchronous processing rate scales according to the current computational load. Additionally, latency is minimized by always updating the MCTS buffer to the latest state where state estimation is possible.

## IV. EXPERIMENTS

We conduct various experiments to validate our systems. Firstly, we ablate our proposed event representation and streamlined network architecture for the keypoint-based pose estimation in Sec. IV-A. We then evaluate OKVIS2-SuperEvent+, AERO-VIS and two baselines on three popular benchmarks in Sec. IV-B. We compare the systems’ nominal accuracy as well as their real-time results on an embedded device. To further demonstrate the capabilities of AERO-VIS, we conduct two more real-world experiments. In Sec. IV-C, we employ our system onboard a UAV with different environmental conditions to achieve closed-loop trajectory following. Finally, we show the system’s robustness in a large-scale handheld experiment and analyze the computation time in Sec. IV-D.

### A. SuperEvent+ & SuperLitE

We adopt the training strategy and relative pose estimation evaluation from the baseline SuperEvent [1]. The area-under-curve (AUC) scores for different rotation error thresholds, along with inference times on an embedded device, are reported in Table I. We benchmark on the Event Camera Datasets [35] captured with an iniVation DAVIS240C event

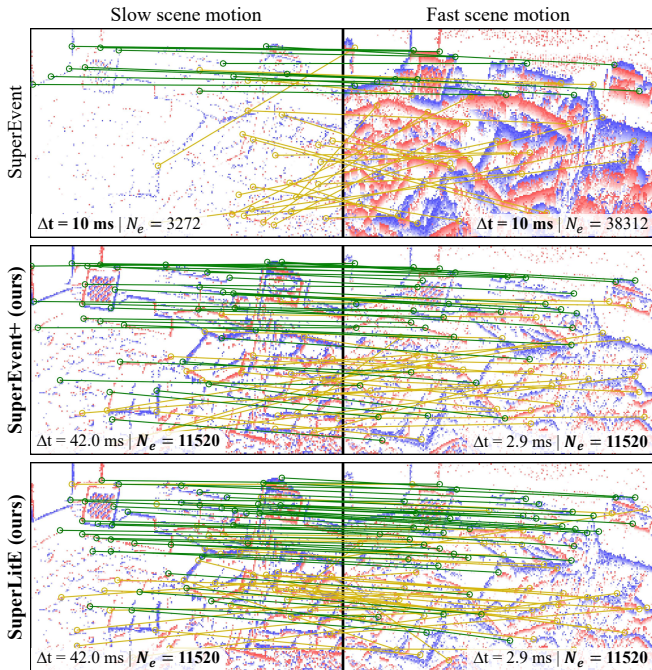


Fig. 3: Two samples of the *boxes\_6dof*-sequence of the ECD dataset: we visualize one channel-pair with positive (red) and negative (blue) polarity for  $MCTS_{\Delta t}$  (fixed time windows) and  $MCTS_{N_e}$  (fixed event counts), as well as the matches predicted by SuperEvent [1], SuperEvent+ and SuperLitE. Green matches have a reprojection error of less than 5 pixels using ground truth pose measurements, while yellow matches are outliers.

TABLE I: Relative pose estimation on Event Camera Dataset (ECD) and Event-aided Direct Sparse Odometry (EDS).

Method	ECD: AUC [%]			EDS: AUC [%]			Infer. time
	@5°	@10°	@20°	@5°	@10°	@20°	
SE [1]	22.7	35.8	46.7	25.3	37.5	48.9	26.2 ms
<b>SE+ (ours)</b>	<b>24.3</b>	<b>40.1</b>	<b>53.3</b>	<b>32.4</b>	<b>47.0</b>	<b>60.2</b>	<b>25.1 ms</b>
<b>SL (ours)</b>	22.3	38.4	52.8	31.2	46.0	59.3	<b>2.5 ms</b>

Area-under-curve (AUC) of SuperEvent (SE) and our variants SuperEvent+ (SE+), and SuperLitE (SL). Inference times of the captured CUDA graph of the TensorRT-compiled models with 16-bit floating-point precision and  $240 \times 400$  pixels input resolution are measured on an NVIDIA Jetson Orin NX.

camera at a  $180 \times 240$  pixel resolution, and the Event-aided Direct Sparse Odometry dataset (EDS) [36] recorded with a Prophesee Gen 3.1 event camera with  $480 \times 640$  pixel resolution.

SuperEvent+ achieves an average relative improvement of 18.7% (AUC @  $10^\circ$ ) over the SuperEvent baseline, driven by our refined MCTS formulation. The inference performance of SuperEvent+ is comparable to the baseline, as the only architectural distinction is the 8-channel input layer – a slight reduction from the baseline’s 10 channels. Our speed-optimized SuperLitE similarly improves the AUC score over the baseline @  $10^\circ$  by 15.0%. However, its inference takes only 2.5 ms which is 90.5% faster than the baseline and 90% faster than SuperEvent+. This enables low-latency state

estimation on compute-restricted onboard devices.

Fig. 3 shows the better adaptability of our  $MCTS_{N_e}$  formulation for motion speed changes. Even though both samples have large visual overlap, the  $MCTS_{\Delta t}$  with constant time windows of SuperEvent result in highly different time surfaces in the 10 ms channel. In contrast, the constant event count  $MCTS_{N_e}$  channel with 0.3 events/pixel is visually more similar. This allows SuperEvent+ and SuperLitE to predict more correct matches that cover a larger area.

## B. Dataset Evaluation

We benchmark our proposed system on three public datasets. The rpg-stereo [37] dataset provides small-scale trajectories recorded with two iVation DAVIS240C cameras. During our experiments, we found a temporal misalignment between the sensor data and pose ground truth. Therefore, we offline estimate a time offset within  $\pm 100$  ms which minimizes the error for all estimators.

The second dataset, TUM-VIE [38], was recorded with Prophesee Gen4 HD cameras at a  $720 \times 1280$  pixel resolution. Only its small-scale *mocap*-sequences have consistent ground truth poses. The *mocap-shake* sequences exhibit aggressive camera shaking and partially featureless views, making estimation highly challenging.

Finally, we benchmark on the large-scale sequences of the VECtor [39] dataset. It employs Prophesee Gen3 CD cameras with  $480 \times 640$  pixels. The indoor sequences contain few and similar features. Vignetting artifacts from the infrared (IR) filter and an imprecise extrinsic calibration of the event cameras introduce additional challenges. Since we were unable to obtain a set of calibration parameters that reliably works on all sequences, we enable the online extrinsic calibration inherited from OKVIS2.

Our SLAM framework offers configurable operating modes: an accuracy-optimized setting for post-processing recorded data, and a performance-oriented setting for real-time applications. To achieve maximum accuracy in offline processing, we employ the full SuperEvent+ network integrated into OKVIS2 with all runtime-related optimizations disabled – including asynchronous processing, which is imposed by real-time constraints. Instead, the synchronous processing rate is set to 50 Hz for small-scale datasets (rpg-stereo and TUM-VIE) and 20 Hz for the large-scale sequences in VECtor. We use a desktop PC with an Intel Core i5-13600 processor, an NVIDIA GeForce GTX 4070 GPU, and 32 GB RAM.

To validate AERO-VIS’s robustness for onboard applications, we evaluate it on an NVIDIA Jetson Orin NX with enforced asynchronous real-time processing. We employ the performance-optimized SuperLitE quantized to 16-bit floating-point precision, compiled by TensorRT, and with CUDA graph capture. Additionally, we limit the maximum number of iterations and the time budget in the backend optimization. We spatially downsample the event stream to a lower resolution to align with the hardware’s real-time processing bandwidth.

TABLE II: Root mean square (RMS) of absolute trajectory error (ATE) [cm]

Dataset	Sequence	Desktop w/o time constraints			NVIDIA Jetson Orin NX in real-time		
		ESVO2 [2]	SDEVO [3]	OKVIS2-SE+ (ours)	ESVO2 [2]	SDEVO [3]	AERO-VIS (ours)
rpg-stereo	bin	3.73 (1.63)	3.78 (4.64)	<b>0.56 (0.41)</b>	216.71	4.27	<b>1.43</b>
	boxes2	8.65 (3.57)	3.50 (0.99)	<b>1.60 (1.08)</b>	734.37	23.14	<b>2.86</b>
	desk2	44.42 (3.27)	5.56 (0.59)	<b>0.81 (0.35)</b>	61.98	27.46	<b>1.26</b>
	monitor2	1.87 (1.80)	2.73 (2.52)	<b>0.60 (0.50)</b>	2.33	3.08	<b>1.30</b>
	reader	123.82 (1.80)	1.59 (0.53)	<b>0.83 (0.48)</b>	102.02	6.44	<b>2.31</b>
TUM-VIE	1d-trans	2.19	1.10	<b>0.34</b>	failed	1.82	<b>1.48</b>
	3d-trans	14.45	1.39	<b>0.65</b>	failed	23.04	<b>0.89</b>
	6dof	3.48	2.22	<b>0.38</b>	failed	4.38	<b>1.05</b>
	desk	9.14	2.52	<b>0.36</b>	failed	18.56	<b>1.18</b>
	desk2	8.73	2.06	<b>0.31</b>	failed	18.47	<b>0.71</b>
	shake	failed	76.55	<b>3.79</b>	failed	91.61	<b>8.13</b>
	shake2	failed	59.09	<b>9.15</b>	failed	73.64	<b>13.46</b>
VECTor	corr.-dolly	failed	126.61	<b>73.28</b>	failed	352.92	<b>174.55</b>
	corr.-walk	failed	331.33	<b>70.22</b>	failed	290.12	<b>237.36</b>
	school-dolly	1448.08	101.46	<b>74.51</b>	failed	247.86	281.45
	school-scooter	failed	824.45	<b>174.44</b>	failed	612.34	<b>256.20</b>
	units-dolly	failed	474.20	<b>136.72</b>	failed	564.34	<b>207.08</b>
	units-scooter	failed	1530.22	<b>138.48</b>	failed	2828.34	<b>326.76</b>

All results are the median of 5 runs. If a system crashes or diverges in at least 3 runs per sequence, we mark it as "failed". Numbers in brackets are corresponding to the cropped sequences used for evaluation in [2], [3]. OKVIS2-SE+ is the event-based version of OKVIS2 with our integrated SuperEvent+. AERO-VIS is our asynchronous extension that employs the faster SuperLitE. We downsample the event streams to  $240 \times 424$  pixels (TUM-VIE) and  $240 \times 320$  (VECTor) for the evaluation on the Jetson Orin NX.

TABLE III: RMS of ATE [cm] for indoor drone experiments.

Type of movement	Lightning condition	Control mode	OKVIS2 [6] (frame-based)	AERO-VIS
"8" shape	normal	closed-loop	<b>2.14</b>	10.83
In-place rot.	HDR	closed-loop	failed*	<b>25.53</b>
Aggressive	normal	handheld	78.08	<b>7.78</b>

\*Drone crashed after large drift.

We compare the results of our two system variants with the two SOTA baselines: the stereo event-inertial ESVO2 [2] and the stereo event-based SDEVO [3]. Both report real-time capability (on a Desktop PC) in their publications. For a fair comparison, we evaluate the baselines on the same hardware and at the same spatial resolutions as our systems. While [5] is also relevant for our evaluation, its source code has not been released publicly, and the system was not benchmarked on public datasets.

Even without real-time constraints, the baseline ESVO2 fails in scenes with high optical flow (e.g., TUM-VIE mocap-shake & -shake2, and VECTor sequences) but also has inconsistent results on the other sequences. The second baseline, SDEVO, achieves better results on most sequences while having large errors on others (e.g., rpg-stereo desk2, TUM-VIE mocap-shake & -shake2, VECTor school-scooter & units-scooter). This lack of robustness could be caused by a domain shift compared to its training data or the missing integration of IMU measurements. OKVIS2-SuperEvent+ achieves the best results on all sequences. This can be attributed to the reliable keypoint detection and description of SuperEvent+ as well as OKVIS2's sophisticated sensor fusion and backend optimization.

In the real-time evaluations on the Jetson Orin NX, ESVO2 exhibits significant instability, characterized by failure or

severe drift across most sequences. These results suggest its computational demands exceed the capabilities of the onboard hardware. The accuracy of SDEVO is constrained by its low inference speed (1–3 Hz), leading to substantial estimation errors across most test sequences. AERO-VIS, however, achieves precise results and – on most sequences – even outperforms ESVO2 and SDEVO's unconstrained desktop results. Crucially, AERO-VIS is the *only* evaluated system capable of reliable onboard state estimation.

### C. UAV Onboard Estimation

To validate AERO-VIS's performance in real-world scenarios and its potential for applications such as drone control, we employ the system on a custom-built UAV. The platform features an NVIDIA Jetson Orin NX, two Prophesee EVK4 event cameras, and a Bosch BMI160 IMU. The stereo configuration utilizes a 7.4 cm baseline and  $110^\circ$  FOV lenses, equipped with IR filters to prevent interference with the motion-capture system. To allow robust online event processing, we spatially downsample the event stream to  $240 \times 424$  pixels on the hardware and additionally restrict the maximum event rate to 35 MEV/s. As a drone controller, we use a linear MPC [40] to follow predefined trajectories.

We evaluate three different scenarios. Firstly, we employ AERO-VIS with closed-loop control in a well-lit environment to execute a trajectory of an "8"-shape five times, covering an area of  $\sim 5 \text{ m}^2$ . For the second scenario, we turn off the lights and place a light source behind a window to test the system's robustness to HDR. Again, the UAV is controlled by AERO-VIS's real-time estimation to spin 10 times in place. Finally, we simulate aggressive flight with a handheld shake of the drone in the horizontal plane and rapid

rotation around its vertical axis. We measure ground-truth trajectories using a motion-capture system to evaluate our system’s accuracy. As a baseline, the original OKVIS2 [6] is evaluated in the same experiments using the frame camera RealSense 455 with a  $480 \times 640$  pixel resolution and the integrated Bosch BMI055 IMU.

Table III lists the resulting trajectory estimation errors in the different experiments, and Fig. 1 shows the estimated and measured trajectories. Under normal conditions, OKVIS2 outperforms AERO-VIS. The precision of AERO-VIS is limited by reduced spatial resolution and sensitivity of time surfaces to vibration-induced appearance changes. These factors introduce additional challenges for the event-based system compared to frame-based perception. However, the other two experiments demonstrate the event camera’s increased robustness to HDR and rapid motion. In the HDR experiment, the estimate of AERO-VIS drifts by  $\sim 1$  m. We identified rotation-only trajectories as a constraint for OKVIS2’s loop closure detection. Since the system enforces a bound on the maximum relative linear drift, the lack of significant translational movement effectively prevents loop-closure triggers. Still, AERO-VIS demonstrates superior stability compared to the frame-based baseline. While both systems experience drift, the error magnitude of OKVIS2 is substantially higher, causing the UAV to crash into the wall after 5 rotations. In the third experiment simulating aggressive flight, AERO-VIS reduces the estimation error by 90% compared to frame-based OKVIS2 due to the event camera’s higher temporal resolution and lower sensitivity to motion blur, resulting in significantly less drift.

#### D. Large-scale Real-world Loop

Finally, we qualitatively analyze AERO-VIS in a large-scale real-world experiment. We use the same hardware setup as described in Sec. IV-C and walk a loop of 2 km in 20 min in an urban environment containing various lighting conditions (sun, shade, artificial light) and dynamic entities (cars, pedestrians, bicycles). The online-estimated trajectory is overlaid on a satellite image in Fig. 4. In the absence of ground truth, the qualitative accuracy of the system is evident through the close correspondence between the trajectory estimation and the actual street layout. AERO-VIS’s drift remains within 1–2% of the distance traveled and is largely corrected upon loop closure detection. This experiment further shows our system’s robustness and its relevance to real-world robotics.

Table IV lists the evolving timings of several system components. The per-iteration runtime of our proposed extensions – MCTS preparation and the keypoint detection – is nearly constant throughout the experiment. The keypoint detection timing combines SuperLitE inference, non-maximum suppression, descriptor interpolation from the lower-resolution output map, and descriptor quantization. As the trajectory length increases, the loop closure detection becomes a significant bottleneck. Keypoint matching and backend optimization also contribute to rising overhead over



Fig. 4: Estimated trajectory during a 2 km (20 min) urban walk, processed online on an NVIDIA Jetson Orin NX. The initial pose was manually aligned with the map.

TABLE IV: Mean cycle time of AERO-VIS’s components during the large-scale real-world experiment [ms].

Time interval [min]	0 – 5	5 – 10	10 – 15	15 – 20
MCTS Preparation <sup>1,2</sup>	10.2	9.6	9.3	9.3
Keypoint detection <sup>2</sup>	14.3	13.7	13.4	13.2
Matching & filtering	27.6	42.2	45.0	48.9
Loop closure detection	18.6	67.3	96.9	106.2
Backend optimization <sup>2</sup>	21.9	31.8	38.0	43.2
Other <sup>3</sup>	16.1	15.0	16.6	15.4
Total cycle time	84.2	156.3	196.5	213.7

<sup>1</sup>Runs in 50 Hz real-time thread. <sup>2</sup>Run in parallel.

<sup>3</sup>Auxiliary tasks, inter-process communication, memory management.

time. Since these limitations are inherent to the integrated OKVIS2 framework and persist in the original system’s frame-based processing, we consider the optimization of these components to be outside the scope of this paper. However, even when processing rates drop below 5 Hz, AERO-VIS reliably estimates the trajectory.

## V. CONCLUSION

We presented AERO-VIS, an event-inertial SLAM system that integrates our performance-optimized keypoint detection and description network, SuperLitE, into our asynchronous version of OKVIS2, tailored for onboard event processing. Even with severely restricted computational resources, it outperforms current SOTA results obtained without these restrictions.

We additionally conduct several real-world experiments. Firstly, we demonstrate closed-loop UAV control by onboard event-based state estimation. Secondly, AERO-VIS outperforms the original frame-based OKVIS2 in HDR and aggressive motion scenarios. Finally, our system produces accurate estimates over a long time horizon and reliably detects loop closures.

While AERO-VIS pushes the boundaries of onboard event-based estimation, UAV vibrations appear to degrade its accuracy. Under standard flight conditions, a performance gap remains relative to the frame-based OKVIS2. By efficiently merging event-based keypoint detections with other modalities, such as frames or LiDAR, a hybrid system could potentially achieve the high accuracy of OKVIS2 alongside the robustness to HDR and fast motion of AERO-VIS.

Ultimately, AERO-VIS demonstrates that asynchronous event-inertial SLAM can meet the demands of onboard UAV control. By addressing the trade-off between low-latency sensing and estimation precision, this work provides a viable path for autonomous navigation in environments where traditional vision fails.

#### ACKNOWLEDGEMENT

We thank Rhythm Chandak for her efforts in hardware integration, as well as Cédric Le Gentil and Leonard Diederich for providing valuable feedback on the manuscript.

#### REFERENCES

- [1] Y. Burkhardt, S. Schaefer, and S. Leutenegger, "Superevent: Cross-modal learning of event-based keypoint detection for slam," in *Proceedings of the IEEE/CVF International Conference on Computer Vision (ICCV)*, 2025.
- [2] J. Niu, S. Zhong, X. Lu, S. Shen, G. Gallego, and Y. Zhou, "ESVO2: Direct visual-inertial odometry with stereo event cameras," *IEEE Transactions on Robotics*, 2025.
- [3] S. Zhong, J. Niu, and Y. Zhou, "Deep visual odometry for stereo event cameras," *IEEE Robotics and Automation Letters*, 2025.
- [4] P. Chen, W. Guan, and P. Lu, "ESVIO: Event-based stereo visual inertial odometry," *IEEE Robotics and Automation Letters*, 2023.
- [5] D. Tejero-Ruiz, D. Solís-Martín, F. J. Pérez-Grau, and J. Borrego-Díaz, "Indoor UAV navigation using event cameras and intermediate frame reconstruction," *Computer Vision and Image Understanding*, 2026.
- [6] S. Leutenegger, "OKVIS2: Realtime scalable visual-inertial SLAM with loop closure," *arXiv preprint*, 2022.
- [7] A. Z. Zhu, N. Atanasov, and K. Daniilidis, "Event-based visual inertial odometry," in *2017 IEEE Conference on Computer Vision and Pattern Recognition (CVPR)*, 2017.
- [8] A. Hadviger, I. Cvišić, I. Marković, S. Vražić, and I. Petrović, "Feature-based event stereo visual odometry," in *2021 European Conference on Mobile Robots (ECMR)*, 2021.
- [9] X. Lagorce, G. Orchard, F. Galluppi, B. E. Shi, and R. B. Benosman, "HOTS: A hierarchy of event-based time-surfaces for pattern recognition," *IEEE Transactions on Pattern Analysis and Machine Intelligence*, 2017.
- [10] I. Alzugaray and M. Chli, "Asynchronous corner detection and tracking for event cameras in real time," *IEEE Robotics and Automation Letters*, 2018.
- [11] W. Chamorro, J. Sola, and J. Andrade-Cetto, "Event-based line slam in real-time," *IEEE Robotics and Automation Letters*, 2022.
- [12] H. Rebecq, G. Gallego, E. Mueggler, and D. Scaramuzza, "EMVS: Event-based multi-view stereo—3D reconstruction with an event camera in real-time," *International Journal of Computer Vision*, 2018.
- [13] W. Guan and P. Lu, "Monocular event visual inertial odometry based on event-corner using sliding windows graph-based optimization," in *2022 IEEE/RSJ International Conference on Intelligent Robots and Systems (IROS)*, 2022.
- [14] B. D. Lucas and T. Kanade, "An iterative image registration technique with an application to stereo vision," in *IJCAI'81: 7th international joint conference on Artificial intelligence*, 1981.
- [15] H. Kim, S. Leutenegger, and A. J. Davison, "Real-time 3D reconstruction and 6-dof tracking with an event camera," in *European conference on computer vision*, 2016.
- [16] H. Rebecq, T. Horstschäfer, G. Gallego, and D. Scaramuzza, "EVO: A geometric approach to event-based 6-dof parallel tracking and mapping in real time," *IEEE Robotics and Automation Letters*, 2016.
- [17] S. Ghosh, V. Cavinato, and G. Gallego, "ES-PTAM: Event-based stereo parallel tracking and mapping," in *European Conference on Computer Vision (ECCV) Workshops*, 2024.
- [18] S. Ghosh and G. Gallego, "Multi-event-camera depth estimation and outlier rejection by refocused events fusion," *Advanced Intelligent Systems*, 2022.
- [19] Y. Zhou, G. Gallego, and S. Shen, "Event-based stereo visual odometry," *IEEE Transactions on Robotics*, 2021.
- [20] Z. Liu, D. Shi, R. Li, Y. Zhang, and S. Yang, "T-ESVO: improved event-based stereo visual odometry via adaptive time-surface and truncated signed distance function," *Advanced Intelligent Systems*, 2023.
- [21] Z. Liu, D. Shi, R. Li, and S. Yang, "ESVIO: event-based stereo visual-inertial odometry," *Sensors*, 2023.
- [22] J. Niu, S. Zhong, and Y. Zhou, "IMU-aided event-based stereo visual odometry," in *2024 IEEE International Conference on Robotics and Automation (ICRA)*, 2024.
- [23] C. Ye, A. Mitrokhin, C. Fermüller, J. A. Yorke, and Y. Aloimonos, "Unsupervised learning of dense optical flow, depth and egomotion from sparse event data," *arXiv preprint*, 2018.
- [24] A. Z. Zhu, L. Yuan, K. Chaney, and K. Daniilidis, "Unsupervised event-based learning of optical flow, depth, and egomotion," in *Proceedings of the IEEE/CVF conference on computer vision and pattern recognition*, 2019.
- [25] S. Klenk, M. Motzet, L. Koestler, and D. Cremers, "Deep event visual odometry," in *2024 International Conference on 3D Vision (3DV)*, 2024.
- [26] Z. Teed, L. Lipson, and J. Deng, "Deep patch visual odometry," *Advances in Neural Information Processing Systems*, 2023.
- [27] W. Guan, F. Lin, P. Chen, and P. Lu, "DEIO: Deep event inertial odometry," in *Proceedings of the IEEE/CVF International Conference on Computer Vision (ICCV) Workshops*, 2025.
- [28] C. Scheerlinck, H. Rebecq, D. Gehrig, N. Barnes, R. Mahony, and D. Scaramuzza, "Fast image reconstruction with an event camera," in *Proceedings of the IEEE/CVF winter conference on applications of computer vision*, 2020.
- [29] P. Geneva, K. Eickenhoff, W. Lee, Y. Yang, and G. Huang, "OpenVINS: A research platform for visual-inertial estimation," in *2020 IEEE International Conference on Robotics and Automation (ICRA)*, 2020.
- [30] D. DeTone, T. Malisiewicz, and A. Rabinovich, "SuperPoint: Self-supervised interest point detection and description," in *Proceedings of the IEEE conference on computer vision and pattern recognition workshops*, 2018.
- [31] Z. Tu, H. Talebi, H. Zhang, F. Yang, P. Milanfar, A. Bovik, and Y. Li, "MaxViT: Multi-axis vision transformer," in *European conference on computer vision*, 2022.
- [32] K. Simonyan, "Very deep convolutional networks for large-scale image recognition," *arXiv preprint*, 2014.
- [33] A. Howard, M. Sandler, G. Chu, L.-C. Chen, B. Chen, M. Tan, W. Wang, Y. Zhu, R. Pang, V. Vasudevan, Q. V. Le, and H. Adam, "Searching for MobileNetV3," in *Proceedings of the IEEE/CVF International Conference on Computer Vision (ICCV)*, 2019.
- [34] D. Gálvez-López and J. D. Tardos, "Bags of binary words for fast place recognition in image sequences," *IEEE Transactions on robotics*, 2012.
- [35] E. Mueggler, H. Rebecq, G. Gallego, T. Delbruck, and D. Scaramuzza, "The event-camera dataset and simulator: Event-based data for pose estimation, visual odometry, and slam," *The International Journal of Robotics Research*, 2017.
- [36] J. Hidalgo-Carrió, G. Gallego, and D. Scaramuzza, "Event-aided direct sparse odometry," in *Proceedings of the IEEE/CVF Conference on Computer Vision and Pattern Recognition*, 2022.
- [37] Y. Zhou, G. Gallego, H. Rebecq, L. Kneip, H. Li, and D. Scaramuzza, "Semi-dense 3D reconstruction with a stereo event camera," in *Proceedings of the European Conference on Computer Vision*, 2018.
- [38] S. Klenk, J. Chui, N. Demmel, and D. Cremers, "TUM-VIE: The TUM stereo visual-inertial event dataset," in *2021 IEEE/RSJ International Conference on Intelligent Robots and Systems (IROS)*, 2021.
- [39] L. Gao, Y. Liang, J. Yang, S. Wu, C. Wang, J. Chen, and L. Kneip, "VECTor: A versatile event-centric benchmark for multi-sensor SLAM," *IEEE Robotics and Automation Letters*, 2022.
- [40] D. Tzoumanikas, W. Li, M. Grimm, K. Zhang, M. Kovac, and S. Leutenegger, "Fully autonomous micro air vehicle flight and landing on a moving target using visual-inertial estimation and model-predictive control," *Journal of Field Robotics*, 2019.